Second-harmonic microscopy of single micrometer-size particles on a substrate

N. Yang, W. E. Angerer, and A. G. Yodh
Department of Physics & Astronomy, University of Pennsylvania, Philadelphia, Pennsylvania 19104-6396
(Received 9 March 2001; published 10 September 2001)

We report experimental observations of second-harmonic generation (SHG) from single micrometer-size polystyrene, silica, and polymethylmethacrylate spheres on flat substrates by SHG microscopy. At low input light intensities the SH signals depend quadratically on the intensity of the excitation beam, but at larger input intensities some of the SH signals increase exponentially with increasing input intensity. This exponential enhancement depends on particle size and sphere composition. We describe the experiments, and parametrize the observations.

DOI: 10.1103/PhysRevA.64.045801 PACS number(s): 42.65.−k, 78.70.−g, 42.25.−p

The linear optical properties of micrometer-size spherical particles have been understood for many years [1,2] and currently provide the basis for characterization of a wide variety of particle dispersions ranging from colloids and emulsions to cells. More recently, the nonlinear optical and lasing properties of spheres have commanded attention [3–6]. These latter phenomena derive their interest in part from unusual cavity effects, and in part because of their potential for material characterization. For example, recent studies of second-harmonic generation (SHG) from colloidal suspensions [7] suggest additional ways to characterize particle surfaces in solution. Further investigation of the fundamental origin of these signals and their phenomenology is desirable, and may lead to additional SHG applications.

The experiments presented in this Brief Report were stimulated by the observations of SHG from colloids [7–10], and by reports of SHG microscopy [11–16]. We have built a scanning SHG microscope, and have used it to study the responses of single colloidal spheres on a flat substrate. We report what we believe to be the first measurements of SHG from *single* micrometer-size particles, and we compare their nonlinear responses over a range of particle type [e.g., polystyrene (PS), polymethylmethacrylate (PMMA), and silica] and size (e.g., diameters between 1 and 5 μm). The measurements provide a benchmark for single-particle SHG signal size, and demonstrate the potential to select and study isolated particles, which might, for example, have different shapes or chemical compositions. At relatively low input powers, the particle SHG signals depend on the square of the fundamental excitation beam intensity. At higher input powers, however, reversible exponential SHG responses are observed from many of the particles up to the point where the signal saturates and the particle is damaged. The precise origin of these exponential responses is not known. One plausible explanation is that the exponential growth of SHG originates from a multiphoton-excitation-induced plasma, whose production is perhaps enhanced further by particle cavity effects. This exponential SH response can, in principle, be used to improve the contrast of a particle in the SHG microscope image.

The goal of this paper is to provide a brief report of our observations. A complete theoretical explanation of the results is beyond the scope of this paper. It would require extensive numerical analysis, which must incorporate the nonparaxial beam optics of the microscope geometry, and nonlinear optical particle cavity effects. Comparison to theory should be possible in the future, however, as theoretical work in the field progresses [17].

Our experiments were performed using a 76 MHz train of ultrashort light pulses derived from a mode-locked Ti:Al_2O_3 laser operating at 840 nm. The apparatus is sketched schematically in Fig. 1(a). A high numerical aperture microscope objective (i.e., 0.85 unless otherwise specified) focuses the nearly Gaussian beam to a spot on the glass substrate with diameter of ~ 1.8 μm; the diameter is defined as the full width at e^{-2} of the intensity maximum. Pulses emerging from the laser had a duration of ~ 100 fsec, but were temporally broadened by the microscope optics to ~ 350 fsec. The laser pulse peak powers at the sample surface ranged from 3 to 36 GW/cm^2.

The sample consisted of a glass substrate in air, sparsely covered with micrometer-size spheres. The sample was raster scanned in the plane normal to the incident beam direction. SH photons collected in remission were spectrally filtered from the fundamental beam, and were measured with a pho-

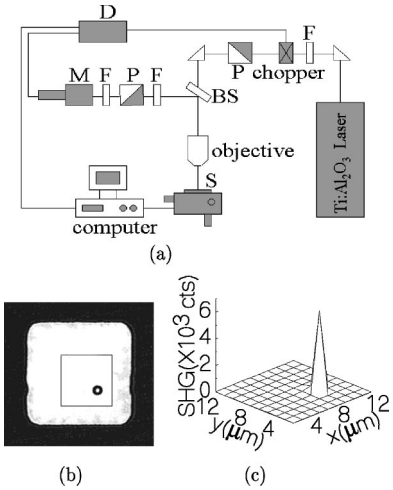

FIG. 1. (a) Schematic view of experimental setup. The sample is mounted on a stepper-controlled x,y,z translation stage. *F*, spectral filter; *P*, prism; BS, beam splitter; *S*, sample; *M*, monochromator; *D*, photon counter. (b) A typical view of the sample. Shown, is a PS particle of 2.19 μm diameter. (c) SHG photons in 5 sec collection time as function of laser spot on the sample of Fig. 1(b).

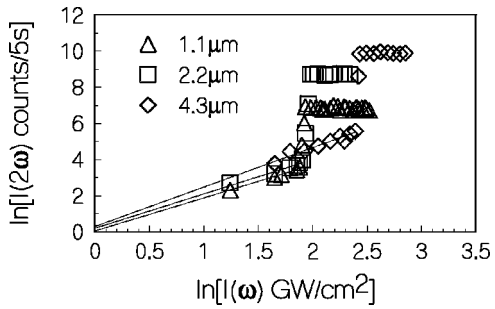

FIG. 2. SHG from PS beads vs input peak intensity for three different sized particles. The solid lines are quadratic fitting. The coefficients for 1.1, 2.2, and 4.3 μm are 1.83, 1.90, and 2.18, respectively.

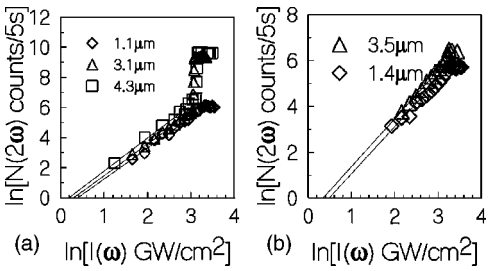

FIG. 3. (a) SHG from PMMA beads versus input peak intensity for three different sized particles. The solid lines are quadratic fitting. The coefficients for 1.1, 3.1, and 4.3 μm are 2.05, 2.10, and 2.19, respectively. (b) SHG from silica bead vs input peak intensity for 1.40 μm and 3.50 μm particles. The solid lines are quadratic fittings. The coefficients for 1.40 and 3.50 μm are 2.05 and 2.09, respectively.

tomultiplier tube coupled to a lock-in photon counter. A charge-coupled device (CCD) camera and monitor were used for sample alignment. The input beam was *p* polarized. The *p*- and *s*-polarized reflected SH outputs were found experimentally to exhibit approximately the same behavior with respect to input power, particle size, and particle type. For the experiments presented herein, our output detector was set to collect *s*-polarized SH photons. All reflected photons whose backscattered angle fell within the numerical aperture of the microscope objective were collected.

In Fig. 1(b) we show the geometry of a typical 25 μm$\times$25 μm scan region along the substrate surface, and in Fig. 1(c) we show the corresponding SHG image taken within a 12 μm $\times$12 μm subset of this sample surface. The particle used [i.e., the the dark spot in Fig. 1(b)] was a 2.19 μm diameter PS sphere, and the input pulse peak intensity was $\sim$7.5 GW/cm^2. The SHG signal from the particle was $\sim 10^3$ times larger than the signal from the glass substrate. This enormous enhancement suggests the technique may have applications in the context of nonlinear optical microscopy.

The essential features of the observed phenomena are depicted in Fig. 2, which shows the SH response of three PS spheres of different diameters (1.1,2.2,4.3 μm) as a function of input pulse peak intensity. The data divide naturally into three regimes. At low peak intensity all particles respond quadratically. Then, as the input intensity is increased, a threshold is reached; at this point the SH signals increase exponentially and finally saturate. The measurements were generally *reversible* up to the saturation point. Permanent bead damage occurred at higher peak powers. In Figs. 3(a) and 3(b) we show the results of similar measurements performed on the PMMA and silica (SiO_2) spheres. Notice that signal saturation was observed for all particles, but exponential signal variation was not exhibited by the smaller spheres, i.e., by the 1.1 μm (1.4 μm) diameter PMMA (silica) particles. We performed similar measurements using an objective with numerical aperture of 0.6. The observed features were qualitatively similar; some differences in input threshold and saturation powers were observed, but they scaled with the expected spot size variation and the simple overlap effects outlined below.

We will not attempt a detailed theoretical analysis of the data. However, we crudely parametrize our observations so that certain general features are made more evident. First consider results in the low input intensity regime. We adopt a very simple model for our analysis. We fit the data assuming

$$I(2\omega) = |\chi^{(2)}_{eff}|^2 [I(\omega)]^m. \tag{1}$$

Here $I(2\omega)$ is the SHG intensity, and $I(\omega)$ is the intensity of the input beam. We allow for the possibility that the exponent m can differ from 2 in our fits. $\chi^{(2)}_{eff}$ is the effective second-order nonlinear susceptibility of the particle. Generally $\chi^{(2)}_{eff}$ will depend in a complicated way on particle optical properties and size, on input beam excitation geometry, and on excitation and emission wavelengths. We assume that the effective susceptibility depends on the product of three factors: (1) an intrinsic material-dependent second order susceptibility $\alpha^{(2)}_j (j = \mathrm{PS}, \mathrm{PMMA}, \mathrm{SiO_2})$. (2) an effective light excitation overlap area S equal to the particle diameter divided by the excitation beam diameter, and (3) a complex geometrical/Fresnel factor $G_{jkl} (j = \mathrm{PS}, \mathrm{PMMA}, \mathrm{SiO_2}$; k = particle diameter, l = light beam geometry), which depends on light beam and sample geometry, and particle properties; we have written G with three subscripts to emphasize that G will depend on many factors, for example, the particle dielectric constant and size, the light polarization, the particle cavity modes that are excited by the input beam, the excitation geometry, and the collection angle (see, for example, Ref. [17]). For this paper we assume $S = 1$ when the particle diameter is bigger than twice the excitation beam diameter.

The solid lines in Figs. 2 and 3 represent our best fits to the low intensity data. From these lines we deduce m and $\chi^{(2)}_{eff}$ for particles of different size and type. Furthermore, from our assumption that $\chi^{(2)}_{eff,\mathrm{PS}} = GS\alpha^{(2)}_{\mathrm{PS}}$, we can approximately incorporate the effects of differing illumination areas. The results for each particle type and size are given in Table I. We see that $m \approx 2$ in all cases. The measurements did not enable us to distinguish the contributions of the surface dipole and bulk quadrupole moments.

From Table I we see that the effective nonlinear susceptibility $\chi^{(2)}_{eff}$ depends on particle type, but not so much on particle size. For example, for the $\sim$1 μm diameter par-

TABLE I. Fitting parameters for quadratic region.

Type	Diameter (μm)	m	$\lvert\chi^{(2)}_{eff}\rvert^2$	$G/G_{\text{silica},3.5}$[a]
PS	1.1	1.83 ± 0.12	1.05 ± 0.08	2.40 ± 0.17
	2.2	1.90 ± 0.23	1.22 ± 0.34	1.58 ± 0.24
	4.3	2.18 ± 0.21	1.35 ± 0.58	1.66 ± 0.37
PMMA	1.1	2.05 ± 0.06	0.45 ± 0.07	1.57 ± 0.16
	3.1	2.10 ± 0.03	0.53 ± 0.04	1.04 ± 0.08
	4.3	2.19 ± 0.09	0.66 ± 0.17	1.16 ± 0.17
silica	1.4	2.05 ± 0.08	0.38 ± 0.09	1.13 ± 0.15
	3.5	2.09 ± 0.04	0.49 ± 0.06	1

[a]These values are calibrated with respect to S.

ticles, $\chi^{(2)}_{eff,\text{PS}}\approx(1.5\pm0.1)\chi^{(2)}_{eff,\text{PMMA}}\approx(1.6\pm0.2)\chi^{(2)}_{eff,\text{SiO}_2}$. Since S is the same for same size particles, these differences may be a result of different intrinsic material nonlinearities (i.e., $\alpha^{(2)}_j$), or may be due to different local electric field strengths within each particle (i.e., via G). Separate linear optical measurements at the same wavelengths give the index of refraction for these three particles as 1.57, 1.47, and 1.44 respectively. Using these refractive index values, Mie calculations show that the local electric field inside the PS particle is only about 10% stronger than in PMMA and silica under plane wave excitation. Thus differences in $\chi^{(2)}_{eff}$ are probably due to intrinsic material nonlinearities. We can also derive some information about the effects of particle size by considering the PS spheres alone. In this case we normalize for the effective area of excitation (i.e., S), and find $G_{1.1\mu\text{m,PS}}$:$G_{2.2\mu\text{m,PS}}$:$G_{4.3\mu\text{m,PS}}=(1.5\pm0.3)$:1:$(1.1\pm0.3)$. These differences in G are not significant given the measurement error. As a final check we compared the SHG signals in the same geometry with that of bulk PS (e.g., a 60 μm thick film), and bulk silica (e.g., a piece of glass). We found that the SHG signals were comparable to those of beads, in the low input intensity regime.

We next consider the dramatic nonlinear enhancement occurring at higher input light intensities (e.g., $\sim$7.0 GW/cm^2 for 2.2 μm diam PS particles). This effect is seen clearly for all our PS particles, and for the two larger PMMA particles. There is also a hint of the effect in the large silica particle data. In Fig. 4 we exhibit the PS data in this regime on a semilogarithmic plot. The linear variation of the SH signal

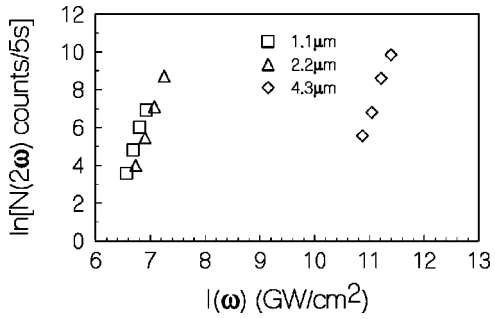

FIG. 4. $\ln(N^{2\omega}_{SHG})$ vs I^{ω} for PS beads showing the exponential growth of the SHG signal in the transition region.

TABLE II. Fitting parameters for transition region.

Type	Diameter (μm)	$\ln A$	α
PS	1.1	-57.69 ± 21.35	9.35 ± 3.17
	2.2	-57.50 ± 21.35	9.13 ± 3.16
	4.3	-86.40 ± 24.45	8.46 ± 2.20
PMMA	3.1	-96.40 ± 33.43	4.86 ± 1.56
	4.3	-121.92 ± 50.31	5.65 ± 2.18

on this plot with respect to input intensity suggests that the enhancement is exponential in the threshold region, i.e.,

$$I(2\omega)=Ae^{\alpha I(\omega)}. \tag{2}$$

In Table II the values of $\ln A$ and α are given for the PS and PMMA particles exhibiting the effect. The silica particle data were too noisy to be analyzed meaningfully. Although there is a large scatter in the value of A, the exponential gain coefficient α is clearly material dependent. It also appears that the threshold for turn-on of the nonlinear enhancements is material dependent and size dependent (see Fig. 4).

The microscopic origin of these exponential enhancements is not readily apparent, although the fact that they occur near the particle damage threshold provides clues about the underlying mechanisms. It is unlikely that these enhancements are driven by conventional, i.e., thermal, laser heating; if the primary material optical absorption is linear, and the subsequent heat losses are diffusive, then we can rule out conventional laser heating damage because the estimated temperature jumps [18] are very small for our laser pulses, and the particle properties would not change enough to induce exponential growth of the SHG signal. On the other hand, one phenomenon that exhibits an exponential dependence with respect to input light intensity is optical breakdown, due to multiphoton excitation/ionization [19]. These multiphoton processes sometimes produce plasmas that at sufficient density can lead to avalanche ionization effects, thus damaging the materials. Just below breakdown, these effects can be reversible (as in our experiment). In this regime, optical properties such as the second-order susceptibility will differ dramatically in the resulting plasma/excited-state compared to the same materials in low excitation. This mechanism might be further enhanced by increased local electric fields within the particle due to its cavity modes. For materials with larger damage thresholds (e.g., silica compared to PMMA, PS), the optical breakdown mechanism would be less likely at the same peak power. There are still other nonlinear effects that can produce similar exponential signal growth. Further work remains to be done to clarify these issues of microscopic origin.

To conclude, we have reported on SHG microscopy of single, micrometer-sized particles in air. Three particle types and several particle sizes were employed. Quadratic and exponential responses were observed, depending on input light intensity. We have parametrized the data with a simple model. The measurements provide benchmarks for signal size and experimental conditions in single-particle SHG ex-

periments. With continued improvements in theory, it should be possible to understand these data more quantitatively.

We are grateful to Alan T. Johnson, Zhiming Yu, Mohammad Islam, Keng-hui Lin, John Crocker, and Jian Zhang for experimental assistance. We also thank Tony Heinz and Harry Tom for stimulating discussions. This work was supported by the NSF through Grant No. DMR-97-01657, and partially by the NSF through the PENN MRSEC, Grant Nos. DMR-00-79909 and DMR-99-71226.

[1] M. Kerker, *The Scattering of Light and Other Electromagnetic Radiation* (Academic Press, New York, 1969).
[2] C.F. Bohren and D.R. Huffman, *Absorption and Scattering of Light by Small Particles* (Wiley, New York, 1983).
[3] R.K. Chang and A.J. Campillo, *Optical Processes In Microcavities* (World Scientific, Singapore, 1996).
[4] S. Qian and R.K. Chang, Phys. Rev. Lett. **56**, 926 (1986).
[5] S.C. Hill and R.E. Benner, J. Opt. Soc. Am. B **3**, 1509 (1986).
[6] S.C. Ching, H.M. Lai, and K. Young, J. Opt. Soc. Am. B **4**, 1995 (1987).
[7] H. Wang, E.C.Y. Yan, E. Borguet, and K.B. Eisenthal, Chem. Phys. Lett. **259**, 15 (1996).
[8] E.C.Y. Yan, Y. Liu, and K.B. Eisenthal, J. Phys. Chem. B **102**, 6331 (1998).
[9] C.S. Yang, H.W. Tom, and M.A. Anderson, Bull. Am. Phys. Soc. **44**, 1580 (1999).
[10] H. Wang, T. Troxler, A.-G. Yeh, and H.-L. Dai, Langmuir **16**, 2475 (2000).
[11] R. Hellwarth and P. Christensen, Opt. Commun. **12**, 318 (1974).
[12] K.A. Schultz, I.I. Suni, and E.G. Seebauer, J. Opt. Soc. Am. B **10**, 546 (1993).
[13] M. Florsheimer, H. Looser, M. Kupfer, and P. Gunter, Thin Solid Films **244**, 1001 (1994).
[14] Y. Uesu, S. Kurimura, and Y. Yamamoto, Appl. Phys. Lett. **66**, 2165 (1995).
[15] V. Kirilyuk, A. Kirilyuk, and T. Rasing, Appl. Phys. Lett. **70**, 2306 (1997).
[16] Y. Guo, P.P. Ho, H. Savage, D. Harris, P. Sacks, S. Schantz, F. Liu, N. Zhadin, and R.R. Alfano, Opt. Lett. **22**, 1323 (1997).
[17] J.I. Dadap, J. Shan, K.B. Eisenthal, and T.F. Heinz, Phys. Rev. Lett. **83**, 4045 (1999).
[18] J.M. Hicks, L.E. Urbach, E.W. Plummer, and H.L. Dai, Phys. Rev. Lett. **61**, 2588 (1988).
[19] Y.R. Shen, *The Principles of Nonlinear Optics* (Wiley, New York, 1984).